

# BEC-BCS Crossover and the Liquid-Gas Phase Transition in Hot and Dense Nuclear Matter

Meng Jin,<sup>1</sup> Michael Urban,<sup>2</sup> and Peter Schuck<sup>2,3</sup>

<sup>1</sup>*Institute of Particle Physics and Physics Department,*

*Hua-Zhong Normal University, Wuhan 4300079, People's Republic of China*

<sup>2</sup>*Institut de Physique Nucléaire, CNRS/IN2P3 and Université Paris-Sud 11, 91406 Orsay Cedex, France*

<sup>3</sup>*Laboratoire de Physique et Modélisation des Milieux Condensés,*

*CNRS and Université Joseph Fourier, BP 166, 38042 Grenoble Cedex, France*

(Dated: May 11, 2010)

The effect of nucleon-nucleon correlations in symmetric nuclear matter at finite temperature is studied beyond BCS theory. Starting from a Hartree-Fock description of nuclear matter with the Gogny effective interaction, we add correlations corresponding to the formation of preformed pairs and scattering states above the superfluid critical temperature within the in-medium  $T$ -matrix approach, which is analogous to the Nozières-Schmitt-Rink theory. We calculate the critical temperature for a BEC superfluid of deuterons, of a BCS superfluid of nucleons, and in the crossover between these limits. The effect of the correlations on thermodynamic properties (equation of state, energy, entropy) and the liquid-gas phase transition is discussed. Our results show that nucleon-nucleon correlations beyond BCS play an important role for the properties of nuclear matter, especially in the low-density region.

PACS numbers: 21.65.-f, 26.60.-c, 64.70.F-

## I. INTRODUCTION

Pairing and nucleon-nucleon correlations are important properties of interacting nuclear systems. For example, in the weak-coupling limit, i.e., at high density, the nucleons form Cooper pairs, and below a certain critical temperature  $T_c$  the system is in a superfluid phase as described by the Bardeen-Cooper-Schrieffer (BCS) theory. In the strong-coupling limit, i.e., at low density, neutrons and protons form deuteron bound states which will condense if the temperature is below the critical temperature for the corresponding Bose-Einstein condensation (BEC). It was theoretically predicted [1] and recently confirmed by experiments with ultracold atomic Fermi gases [2, 3] that there is a smooth crossover between the BCS and BEC limits. Qualitatively, especially at zero temperature, these features can be studied within the BCS (mean field) approximation [4]. Quantitatively, however, the critical temperature obtained in this way is too high because the BCS theory does not include the existence of non-condensed pairs at finite temperature. In order to go beyond mean field, one has to consider pair correlations already above the critical temperature, as in the Nozières-Schmitt-Rink (NSR) theory [1]. Especially in the low density region, where the coupling between nucleons is strong, such correlations modify the mean-field results to a large extent.

At present, there are several groups who have studied nuclear matter within the NSR approach. Pioneering work has been done by the Rostock group [5, 6]. There are also extensions where the correlations are considered in a more self-consistent way, like in the self-consistent Green's function method [7, 8]. A generalization to temperatures below the superfluid transition temperature was discussed by Božek [9]. In the case of ultracold Fermi

gases, where the results can be compared with very precise measurements, theories for the BEC-BCS crossover based on the NSR approach [10] have been very successful [11].

It is well known that there exists a liquid-gas phase transition in nuclear matter. Experimental information can be obtained from multifragmentation (see, e.g., [12–15]). The critical temperature deduced from these experiments depends on the mass of the nuclei and can be as low as 6.7 MeV [15] in the case of small systems. For infinite nuclear matter, theoretical predictions give much higher values for the critical temperature between 14 and 18 MeV [12, 13] (see Ref. [16] for a recent theoretical study). Below that temperature, nuclear matter is unstable in a certain range of low densities. Within mean-field theory, we know that the BCS-BEC crossover is completely covered by the instability region of the liquid-gas phase transition. Nevertheless, the investigation of low-density nuclear matter is of interest for applications where regions of low density appear in the framework of the local-density approximation. Contrary to the nuclear matter case, the whole crossover can be studied in the case of ultracold atomic Fermi gases [2, 3], because the pair correlations stabilize the gas [1] such that the system does not collapse into its solid ground state but it remains in its metastable gas state. By analogy, one expects that pair correlations will stabilize low-density nuclear matter and thus reduce the liquid-gas coexistence region. One of our subjects of investigation will be how strong this effect of nucleon-nucleon correlations on the liquid gas phase transition is quantitatively.

Furthermore, in this paper we will calculate the equation of state of hot and dense symmetric nuclear matter, taking into account the contribution of the mean field together with the nucleon-nucleon correlations. For the

mean field we will use the Gogny interaction because it is known to give a good description of the single-particle and thermodynamic properties of nuclear matter, including saturation at the right density, the liquid-gas phase transition, etc. For the part beyond the mean field, we use the  $T$ -matrix (or ladder approximation) which contains the information on two-particle correlations. This also allows us to extract the critical temperature for pair condensation smoothly interpolating between the BEC and BCS regimes.

The paper is organized as follows. In Sec. II, we will give a summary of the formalism. The numerical results are provided in Sec. III. The last section is devoted to the summary and discussions.

## II. FORMALISM

Before explicitly including two-particle correlations, we calculate the single-particle Green's function within the Hartree-Fock (HF) approximation. In order to get a reasonable description of the single-particle energies, we use the density-dependent D1 Gogny effective interaction to describe the mean field. This force gives nuclear binding at the right saturation point and many other properties of nuclear matter and of finite nuclei [17]. It has the form

$$V(r) = \sum_{m=1}^2 (W_m + B_m P_\sigma - H_m P_\tau - M_m P_\sigma P_\tau) e^{-r^2/\mu_m^2} + t_0(1 + x_0 P_\sigma) \rho^\alpha \delta(r), \quad (1)$$

where the  $P_\sigma$  and  $P_\tau$  are, respectively, the spin and isospin exchange operators. The spin-orbit coupling term is neglected here, since we consider only the properties of infinite nuclear matter. For the parameters we use the values given in Ref. [17] [34]. For details of the HF description of nuclear matter at finite temperature with the Gogny force, see Refs. [18–20]. The HF mean field  $\Sigma_{HF}$  contains the direct, the exchange, and the rearrangement contributions. Because of the finite range of the Gogny force, the exchange contribution is momentum dependent, and the single-particle Green's function takes the form

$$G_{HF}(p, \omega) = \frac{1}{\omega - \xi_p + i0}, \quad (2)$$

where  $\xi_p$  is the quasiparticle energy defined by

$$\xi_p = \frac{p^2}{2m} - \Sigma_{HF}(p) - \mu, \quad (3)$$

where  $\mu$  denotes the chemical potential. In order to facilitate the numerical calculation of the correlation effects, we use the effective-mass approximation for the Gogny mean field, i.e., we write [18]

$$\xi_p = \frac{p^2}{2m^*} - \mu^*. \quad (4)$$

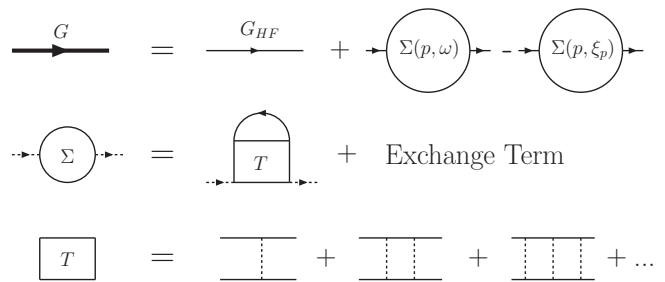


FIG. 1: The Feynman diagrams for the Green's function (top), for the self-energy (middle), and for the  $T$ -matrix in ladder approximation (bottom).

There are different ways to define the effective nucleon mass  $m^*$ . In principle,  $m^*$  is momentum dependent [20]. Here we use the effective mass defined by expanding Eq. (3) around  $p = 0$  (we checked that for the final results it makes almost no difference if we expand around zero or around the Fermi momentum), i.e.,

$$\frac{1}{m^*} = \frac{1}{m} + 2 \left. \frac{d\Sigma_{HF}(p)}{dp^2} \right|_{p=0}, \quad (5)$$

$$\mu^* = \mu - \Sigma_{HF}(0). \quad (6)$$

However, the effective-mass approximation will only be used for the calculation of the correlation effects, while the mean-field contributions will be computed with the full momentum dependence of  $\Sigma_{HF}(p)$ .

In principle, we are looking for the full single-particle Green's function  $G$  including correlations. The Dyson equation can be written as

$$G^{-1}(p, \omega) = G_{HF}^{-1}(p, \omega) - \tilde{\Sigma}(p, \omega), \quad (7)$$

where  $\tilde{\Sigma}$  is the correlation contribution to the single-particle self-energy. Since the Gogny force is a density-dependent effective interaction, which is designed to give good results already at the HF level, we suppose that the Gogny mean field accounts already for most of the correlation effects. We therefore demand that the correlations do not shift the quasiparticle energies  $\xi_p$ , i.e.,  $\tilde{\Sigma}(p, \xi_p) = 0$ , and that the role of the correlations is just to reduce the strength of the quasiparticle pole and to distribute the remaining strength in the continuum of the spectral function. Hence, we define  $\tilde{\Sigma}$  to be the self-energy subtracted at  $\xi_p$ :

$$\tilde{\Sigma}(p, \omega) = \Sigma(p, \omega) - \text{Re} \Sigma(p, \xi_p). \quad (8)$$

In order to describe pair correlations, we calculate the self-energy  $\Sigma$  within the  $T$ -matrix or ladder approximation, as shown in the lower part of Fig. 1. This is a frequently used lowest-order correction [1, 5, 6, 10], implying, however, that vertex corrections as well as screening of the interaction due to the medium effects are neglected.

Since our aim is not a completely self-consistent description of the spectral function as in the self-consistent

Green's function method [7, 8], we make the assumption that the correlations can be treated as a small correction to the Gogny HF self-energy. This allows us to use the HF Green's function  $G_{HF}$  in the calculation of the  $T$  matrix and of the self-energy  $\Sigma$ . Then, for consistency, one should also keep only the first-order term of Eq. (7), i.e.,

$$G(p, \omega) = G_{HF}(p, \omega) + G_{HF}^2(p, \omega) \tilde{\Sigma}(p, \omega). \quad (9)$$

A diagrammatic representation is given in the upper part of Fig. 1

That the self-energy in T-matrix approximation should only be treated in first-order perturbation theory may also have a more formal reason. The T-matrix approximation corresponds to particle-particle random-phase approximation (pp-RPA) [21]. It can be shown that the ground-state energy calculated from the single-particle Green's function with self-energy in first order and in T-matrix approximation yields exactly the pp-RPA ground-state energy [22]. At least this holds true for the self-energy without subtraction procedure. Therefore our formalism is closely related to that of Ref. [23], where the pp-RPA formalism is used, except that we apply the subtraction prescription while the authors of Ref. [23] are obliged to reduce the correlation contribution by introducing a cutoff and to change the parameters of the Gogny force in order maintain the right saturation point of nuclear matter.

Note that our approximations are analogous to NSR theory [1], except that in NSR theory free Green's functions instead of HF ones are used and consequently no subtraction is made in the self-energy. In the case of nuclear matter, however, we cannot expect to obtain a good description of the full self-energy from such a simple model for the  $T$  matrix. This is why we use the Gogny mean field and the subtraction method described above, while the subtracted self-energy serves only to provide the energy dependence corresponding to the pair correlations in the channels we want to study.

In order to get a simple expression for the  $T$  matrix, we use the separable Yamaguchi potential [24],

$$V_\alpha(k, k') = -\lambda_\alpha v(k)v(k') \quad (10)$$

where  $k$  and  $k'$  are the incoming and outgoing relative momenta in the center-of-mass frame, and the form factor is given by

$$v(k) = \frac{1}{k^2 + \beta^2}. \quad (11)$$

As in Ref. [6], we consider only S-wave scattering ( $\alpha = {}^1S_0, {}^3S_1$ ) and neglect the coupling between the  ${}^3S_1$  and  ${}^3D_1$  channels (which comes from the tensor force). With the parameters  $\beta = 1.4488 \text{ fm}^{-1}$ ,  $\lambda_{{}^1S_0} = 2994 \text{ MeV fm}^{-1}$  and  $\lambda_{{}^3S_1} = 4264 \text{ MeV fm}^{-1}$  [6], the low-energy nucleon-nucleon phase shifts and the vacuum binding energy of the deuteron ( $E_b^0 = -2.225 \text{ MeV}$ ) are very well reproduced, see results for  $n = 0$  in Figs. 2 and 3, so that it is unlikely that the coupling between the  ${}^3D_1$  and  ${}^3S_1$

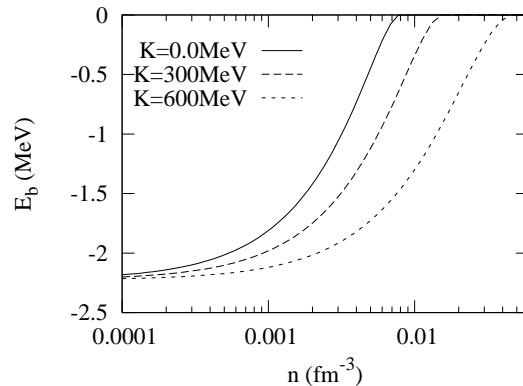


FIG. 2: The deuteron binding energy in nuclear matter from the Yamaguchi potential and including the effect of the Gogny mean field, as a function of the density for different values of the deuteron momentum  $K$ . The temperature is  $T = 10 \text{ MeV}$ .

channels would strongly modify our results. With the separable interaction, the resummation of the ladder diagrams shown in the lower part of Fig. 1 reduces to a simple geometrical series, and the  $T$  matrix can be written as

$$T_\alpha(k, k', K, \omega) = \frac{V_\alpha(k, k')}{1 - J_\alpha(K, \omega)}, \quad (12)$$

where  $\mathbf{k}$  and  $\mathbf{k}'$  are the incoming and outgoing momenta in the center of mass frame,  $\mathbf{K}$  is the total momentum, and

$$J_\alpha(K, \omega) = \int \frac{d^3k}{(2\pi)^3} V_\alpha(k, k) \times \frac{1 - f(\xi_{\mathbf{K}/2+\mathbf{k}}) - f(\xi_{\mathbf{K}/2-\mathbf{k}})}{\omega - \xi_{\mathbf{K}/2+\mathbf{k}} - \xi_{\mathbf{K}/2-\mathbf{k}} + i0}. \quad (13)$$

The function  $f(\xi) = 1/(e^{\xi/T} + 1)$  is the Fermi function,  $T$  being the temperature. Within the effective mass approximation, Eq. (4), the denominator of Eq. (13) does not depend on the angle between  $\mathbf{k}$  and  $\mathbf{K}$ , and the angular integral can be done analytically. The main contribution to the integral over the relative momentum comes from low momenta due to the form factor of the Yamaguchi interaction ( $k \lesssim \beta$ ).

In the  ${}^3S_1$  channel, it can happen that  $J_{{}^3S_1}(K, \omega_b) = 1$  at some energy  $\omega_b$  below the threshold energy

$$\omega_0(K) = \frac{K^2}{4m^*} - 2\mu^*. \quad (14)$$

This means that there is a bound state (the deuteron) with binding energy  $E_b(K) = \omega_b(K) - \omega_0(K)$ . As an example, the deuteron binding energies for different values of the deuteron momentum  $K$  are displayed in Fig. 2. As one can see, the binding gets weaker with increasing density, and eventually the deuteron gets unbound at the so-called Mott density. Since the Pauli blocking

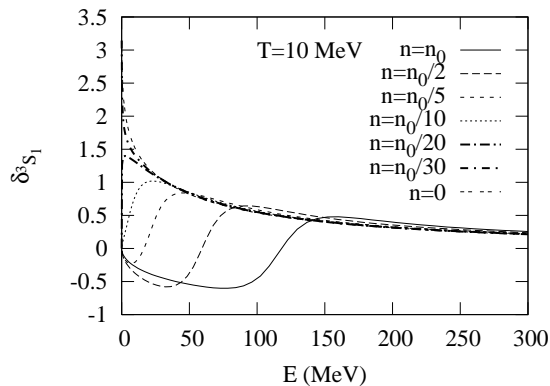


FIG. 3: In-medium scattering phase shift in the  ${}^3S_1$  channel for  $K = 0$  as a function of  $E = k^2/m^*$  for different densities and  $T = 10$  MeV.

effect gets weaker with higher deuteron momentum  $K$ , there exists for any density a Mott momentum  $K_{Mott}$  above which the deuteron stays bound.

The in-medium nucleon-nucleon phase shifts  $\delta_\alpha$  can easily be obtained from  $1/(1 - J_\alpha) = e^{i\delta_\alpha}/|1 - J_\alpha|$ . As an example, we show in Fig. 3 the phase shift in the  ${}^3S_1$  channel for  $K = 0$  at different densities, as function of the energy  $E = \omega + 2\mu^* = k^2/m^*$ . We see that at higher densities, e.g., at  $n \geq n_0/5$  ( $n_0 = 0.17 \text{ fm}^{-3}$  being the saturation density of nuclear matter), the phase shift is negative in the low-energy region and then becomes positive as the energy increases. The energy where the phase shift crosses zero is  $\omega = 0$ , i.e.,  $E = 2\mu^*$ . At lower densities, when  $\mu^*$  is negative, the phase shift is positive at low energy. At some very low density, the value of the phase shift at  $E = 0$  changes from 0 to  $\pi$ . This happens precisely at the density below which the deuteron is bound.

In terms of the  $T$  matrix, we can write the self-energy  $\Sigma$  depicted in the middle of Fig. 1 within the Matsubara formalism as

$$\Sigma(p, i\omega_n) = \frac{3}{2} \sum_{\alpha = {}^3S_1, {}^1S_0} T \sum_{n'} \int \frac{d^3 p'}{(2\pi)^3} G_{HF}(p', i\omega_{n'}) \times T_\alpha(k, k, K, i\omega_n + i\omega_{n'}), \quad (15)$$

where  $\omega_n$  and  $\omega_{n'}$  are Fermionic Matsubara frequencies [ $\omega_n = (2n + 1)\pi T$ ],  $\mathbf{k} = (\mathbf{p} - \mathbf{p}')/2$ , and  $\mathbf{K} = \mathbf{p} + \mathbf{p}'$ . The factor  $3/2$  is the product of a factor  $1/4$  from the averaging over spin and isospin in symmetric nuclear matter, of a factor 2 from the sum of direct and exchange contributions, and of a factor  $(2S + 1)(2T + 1) = 3$  for  $\alpha = {}^3S_1$  and  ${}^1S_0$  from the sum over spin and isospin in the loop. Using standard techniques [25], the self-energy can be analytically continued to real energies, which is necessary for the calculation of the subtraction term  $\Sigma(p, \xi_p)$  in Eq. (8).

Inserting the self-energy into Eq. (9), we calculate the

density from

$$n(T, \mu) = -4T \sum_n \int \frac{d^3 k}{(2\pi)^3} G(k, i\omega_n). \quad (16)$$

The factor 4 comes from the sum over spin and isospin. It is clear that the first term of Eq. (9) just gives the Hartree-Fock density, and the second term gives the correction beyond the mean field approximation. After a lengthy derivation (see Appendix), one finds the following formulas initially given in Refs. [5, 6]:

$$n = n_{HF} + n_{corr} = n_{HF} + n_{bound} + n_{scatt}. \quad (17)$$

The bound-state contribution reads

$$n_{bound} = 6 \int_{K > K_{Mott}} \frac{d^3 K}{(2\pi)^3} g(\omega_b(K)), \quad (18)$$

where  $g(\omega) = 1/(e^{\omega/T} - 1)$  is the Bose function. This term gives the nucleon density corresponding to a Bose gas of deuterons. The scattering-state contribution reads

$$n_{scatt} = -6 \int_{K > K_{Mott}} \frac{d^3 K}{(2\pi)^3} g(\omega_0(K)) - 6 \sum_{\alpha = {}^3S_1, {}^1S_0} \int \frac{d^3 K}{(2\pi)^3} \int_{\omega_0(K)}^\infty \frac{d\omega}{\pi} \left( \frac{d}{d\omega} g(\omega) \right) \times \left( \delta_\alpha - \frac{1}{2} \sin 2\delta_\alpha \right). \quad (19)$$

In Ref. [5], these equations were derived in a different way using the optical theorem, analogously to the derivation of a similar formula for the electron-hole system in Ref. [26].

Note that in spite of the double pole of the derivative of the Bose function at  $\omega = 0$ , the integrand in Eq. (19) has no pole. This is because  $\delta_\alpha$  crosses zero at  $\omega = 0$ . This simple zero is raised to a double one due to the difference of the two terms in the second line of Eq. (19) [35].

Once we have calculated the density, we can calculate the pressure. To that end, we integrate the thermodynamic relation  $n = (dP/d\mu)_T$  over  $\mu$ , i.e.,

$$P(T, \mu) = \int_{-\infty}^\mu n(T, \mu') d\mu'. \quad (20)$$

Then we calculate the free-energy density  $F/V$ , the entropy density  $S/V$ , and the energy density  $E/V$  from the thermodynamic relations

$$F = -PV + \mu nV, \quad S = - \left. \frac{\partial F}{\partial T} \right|_n, \quad \text{and} \quad E = F + TS. \quad (21)$$

### III. NUMERICAL RESULTS

#### A. Density and the superfluid critical temperature

We calculate the total density by numerically integrating Eqs. (18) and (19). The results for the densities

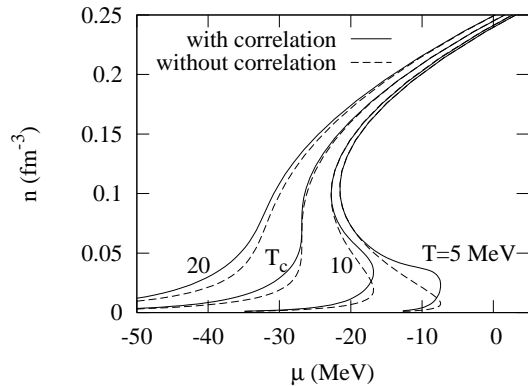


FIG. 4: The densities at  $T = 20, 15.9, 10,$  and  $5$  MeV (from left to right) as functions of the chemical potential within Gogny HF (dashes) and with correlations (solid line).  $T_c^{liq-gas} = 15.9$  MeV is the critical temperature for the liquid-gas phase transition.

at different temperatures as functions of the chemical potential[36] are shown in Fig. 4. Comparing the results with correlations (solid lines) with the Gogny HF results (dashed lines), one can see that, for a given chemical potential, the correlations increase the densities. In the high-density region, we notice that the results with and without correlations converge to the same value, i.e., the correlations fade away at high density, as this can be expected. For example, at  $T = 5$  MeV, the two results coincide starting from  $n = 0.07 \text{ fm}^{-3}$ . This is a consequence of the Mott mechanism, which has been discussed at length in Ref. [5]. As mentioned above, the critical number density where the bound state (at  $K = 0$ ) disappears is called Mott density. When we change the temperature from 5 MeV to 10, 15.9, and 20 MeV, the Mott density changes from  $0.07 \text{ fm}^{-3}$  to 0.12, 0.18, and  $0.22 \text{ fm}^{-3}$ . This means that the mean field approximation is valid in the high density region. Below this region, the contribution of the nucleon-nucleon correlations is important.

From this figure we also can see that when the temperature is less than some critical value ( $T_c^{liq-gas} = 15.9$  MeV), the number density has three values corresponding to one definite value of chemical potential. This is a typical feature of the liquid-gas phase transition in nuclear matter. We will discuss this phenomenon in detail in the next subsection.

To see how large the correlation contribution to the density is, we show the composition of the system at different temperatures in Figs. 5 and 6. Since the density ratios are shown as functions of the density and not of the chemical potential, there are unique solutions even for temperatures below  $T_c^{liq-gas}$ . In Fig. 5 one can see that at  $T = 5$  MeV the correlation contribution to the total density is important at low density ( $n < n_0/4$ ). At  $n = 0.02 \text{ fm}^{-3}$ , the correlated part is even larger than the HF part. This means that most of the nucleons are in correlated pairs in this density region. With increas-

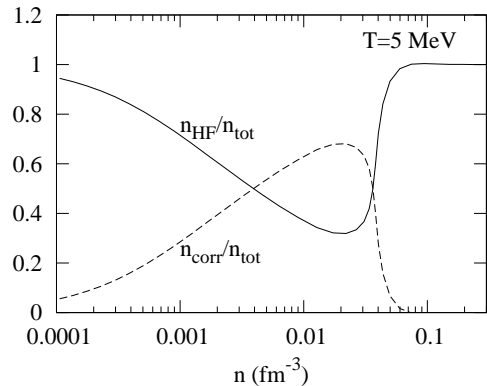


FIG. 5: HF and correlation contributions to the total density  $n_{tot} = n_{HF} + n_{corr}$  for  $T = 5$  MeV.

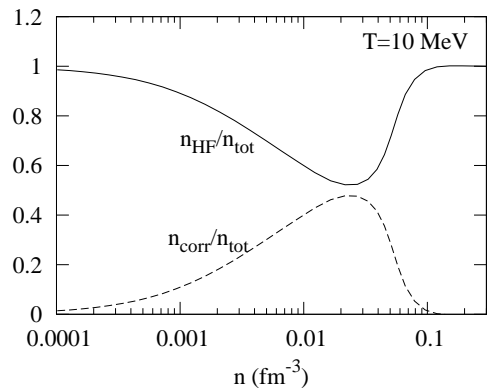


FIG. 6: Same as Fig. 5, but for  $T = 10$  MeV.

ing temperature, e.g., at  $T = 10$  MeV as shown in Fig. 6, the ratio of the correlated density to the total density decreases, but the density region with sizeable nucleon correlations is enlarged. Here we do not separate the correlation contribution into bound and scattering state contributions, since individually they are not very meaningful, as discussed in Ref. [5]. For instance, if the temperature is much higher than the deuteron binding energy, the first term of the scattering-state contribution (19) cancels almost exactly the bound-state contribution (18).

In the above calculation, when the temperature is below some critical value, we get a divergence in the  $T$  matrix. This pole corresponds to the formation of Cooper pairs at high density and to Bose-Einstein condensation of deuterons at low density. Below this critical temperature  $T_c$ , the equations for the density of the system are not applicable any more. In the superfluid phase, one would have to include the nucleon pairing gap explicitly in the single-particle Green's function (which then becomes a  $2 \times 2$  matrix in Nambu-Gorkov space [25]), which is beyond the scope of this paper. However, we can determine the critical temperature of the superfluid transition as the temperature where the  $T$  matrix devel-

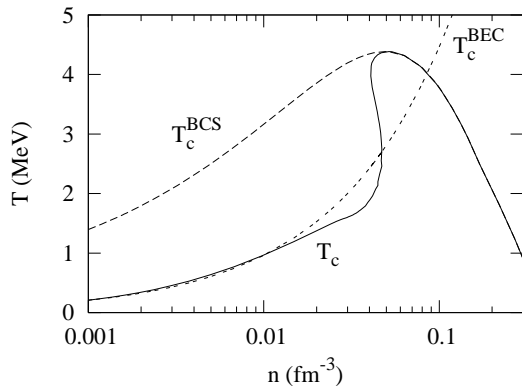


FIG. 7: Superfluid critical temperature as a function of the (total) density. The solid line is the full calculation, while the long dashes correspond to the BCS result. The short dashes show the critical temperature of Bose-Einstein condensation of a deuteron gas.

ops a pole at zero total momentum ( $K = 0$ ) and at zero energy ( $\omega = 0$ ). This is the well-known Thouless criterion [27] for the onset of superfluidity, coinciding with the BCS gap equation when the gap  $\Delta$  goes to zero:

$$1 - J_\alpha(K = 0, \omega = 0; T = T_c) = 0. \quad (22)$$

From this equation we get the critical temperature as a function of the effective chemical potential. Using the relation between the effective chemical potential and the number density, we obtain the superfluid region beyond the BCS (mean field) result as shown in Fig. 7. Qualitatively, this result is similar to the one in [6] except that we have a lower critical temperature for the superfluid phase transition. The maximum  $T_c$  in [6] is 7.2 MeV at  $n = 0.12 \text{ fm}^{-3}$ , while we have  $T_c = 4.5 \text{ MeV}$  at  $n = 0.05 \text{ fm}^{-3}$ . The difference stems from the Gogny mean field, in particular from the effective mass, which was neglected in Ref. [6]. One realizes that a  $T_c$  of 4.5 MeV is still very high, leading to a maximal gap of about 7 MeV, about three times as much as the maximum value of the neutron-neutron gap in the spin singlet channel. The reason clearly stems from the slightly stronger attraction in the proton-neutron isoscalar channel. However, in finite nuclei barely any enhancement of pairing in the  $S = 1, T = 0$  channel can be detected. Probably important screening is at work in that channel. In nuclear matter, this has been investigated in Ref. [31]. The addition of screening effects is, however, beyond the scope of this paper.

As mentioned above,  $T_c$  as a function of  $\mu$  coincides with the BCS result. As a function of the density, the difference between the results  $T_c(n)$  with and without correlations comes only from the different relations for  $n$  as a function of  $\mu$ . Since the correlation contribution to the density vanishes in the high density region, the phase boundary coincides with the BCS curve (long dashed line, which is obtained with  $n_{HF}$  only). At very low density and temperature, the main contribution to

the density comes from the deuteron bound state, as can be seen from Eqs. (17) and (18). Close to the Bose critical temperature, the Bose distribution function in Eq. (18) starts to diverge and, therefore, dominates the whole expression for the density. Therefore the superfluid critical temperature at low density coincides with the critical temperature for Bose-Einstein condensation of a deuteron gas, which is given by

$$T_c^{BEC} = \frac{\pi}{m} \left( \frac{n}{6\zeta(3/2)} \right)^{2/3}, \quad (23)$$

(with  $\zeta(3/2) = 2.612\dots$ ) and is shown as the short-dashed line in Fig. 7.

A surprising behavior of our result is that in the density region between  $0.04 \text{ fm}^{-3}$  and  $0.05 \text{ fm}^{-3}$ , Eq. (22) for the critical temperature has three solutions for one given density. This behavior is not easy to understand from physical intuition. It seems to be related to the effective mass, since it is absent in Ref. [6]. Anyway, as we will show in the next subsection, this density region lies inside the unstable region of the liquid-gas phase transition.

## B. Pressure and liquid-gas transition

As it was shown in Fig. 4, there is a region of densities where the chemical potential decreases with increasing density. This is a typical feature of a liquid-gas phase transition. In order to determine the boundary of this first-order phase transition, we need the pressure. In principle, one can get the pressure as a function of temperature and chemical potential,  $P(T, \mu)$ , from the number density  $n(T, \mu)$  by integration over the chemical potential  $\mu$ , cf. Eq. (20). However, since there is a first-order phase transition,  $n$  is not a single-valued function of  $\mu$  any more. We therefore transform the integral over  $\mu$  into an integral over  $n_{HF}$ :

$$P(T, n_{HF}) = \int_0^{n_{HF}(T, \mu)} n(T, n'_{HF}) \left. \frac{\partial \mu}{\partial n'_{HF}} \right|_T dn'_{HF}. \quad (24)$$

Since  $\mu$  is a single-valued function of  $n_{HF}$  (see dashed line in Fig. 4), this integral is well defined. In this way we obtain the pressure as a function of  $n_{HF}$ , but neither  $n_{HF}$  nor  $P$  are single-valued functions of  $\mu$ .

If we plot the pressure as a function of the total density  $n$  instead of  $n_{HF}$ , we get the results shown in Fig. 8. Unfortunately, we cannot calculate the pressure for  $T < 4.5 \text{ MeV}$ , at least not at densities above  $0.05 \text{ fm}^{-3}$ , because our method to calculate the pressure at a given density  $n$  necessitates the calculation of all densities  $n' < n$ , i.e., including the density at  $n = 0.05 \text{ fm}^{-3}$  where  $T_c$  is maximum. For comparison, we also give the results for the pressure within the mean-field approximation (dashed lines in Fig. 8). As it can be seen, the main effect of the nucleon-nucleon correlations is to increase the pressure at very low densities. However, in the

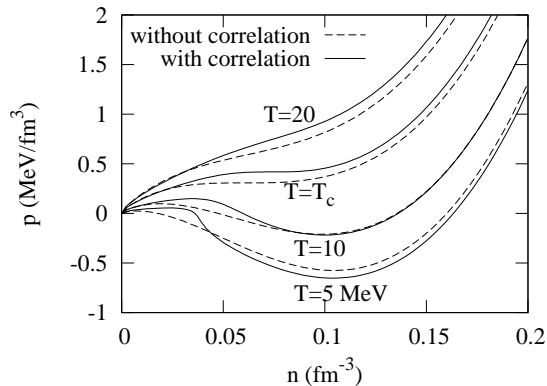


FIG. 8: The pressure as a function of density at different temperatures. Solid lines: with correlations; dashed lines: mean-field results.

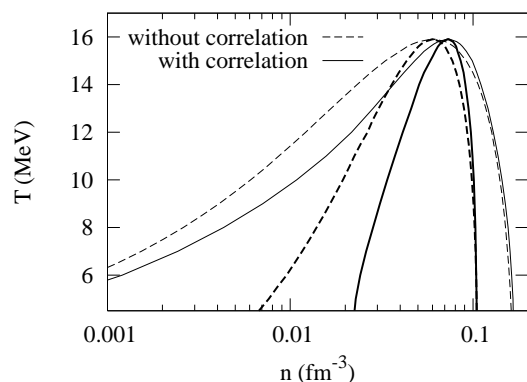


FIG. 9: The liquid-gas phase diagram as function of density and temperature (for  $T \geq 4.5$  MeV). The thin lines are the boundary of the coexistence region, while the thick lines are the boundary of the spinodal region. Solid lines: with correlations; dashed lines: mean field results.

case  $T = 5$  MeV shown in Fig. 8, the pressure at higher densities is lower than the HF result.

Using the pressure, one can determine the coexistence region of the liquid and gas phases of nuclear matter from the following conditions:

$$P(T, n_1) = P(T, n_2) \quad \text{and} \quad \mu(T, n_1) = \mu(T, n_2). \quad (25)$$

The result is shown in Fig. 9 as the thin solid line. At the same time, we can determine the spinodal curve from the zeros of  $\partial P/\partial n$  (or, equivalently, of  $\partial\mu/\partial n$ ), which is shown as the thick solid line in Fig. 9. In the region under the spinodal curve, the system cannot exist in a homogeneous phase. In the region between the thin solid line and the spinodal curve, the gas phase (left-hand part) or the liquid phase (right-hand part) can exist as a metastable state. For comparison, the corresponding mean-field results are presented in Fig. 9 as the dashed lines, which coincide with Fig. 6 of Ref. [20].

Comparing the results with and without correlations, one can see that the correlations decrease the phase-

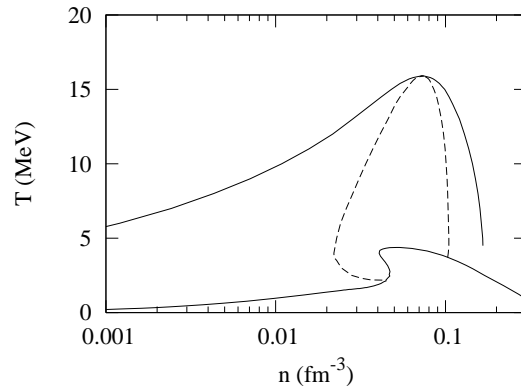


FIG. 10: Phase diagram combining the boundary of the superfluid phase (lower curve), the liquid-gas coexistence region (upper curve), and the spinodal line (dashed curve). The reason why the spinodal and coexistence curves end at  $T_c$  and 4.5 MeV, respectively, is not physical but it simply means that our model does not allow us to compute them at lower temperatures (see text).

transition temperature in the low-density region and reduce the unstable region of the liquid-gas phase transition considerably. As mentioned in the introduction, this is an expected result. In the high density region, the effect of the correlations is almost negligible.

We can determine the critical temperature of the liquid-gas transition, i.e., the maximum temperature of the coexistence and the spinodal curves, from

$$\left. \frac{\partial P}{\partial n} \right|_{T_c^{liq-gas}} = \left. \frac{\partial^2 P}{\partial n^2} \right|_{T_c^{liq-gas}} = 0, \quad (26)$$

see Fig. 8. In this way, we obtain  $T_c^{liq-gas} = 15.9$  MeV, which coincides with the mean-field result [19, 20]. The fact that  $T_c^{liq-gas}$  remains unchanged is an artifact of our present approach to treat the correlation effects only at a perturbative level, as explained in Sec. II. As shown in Ref. [30], the inclusion of deuteron (and heavier) clusters should reduce the liquid-gas critical temperature. We would have to do the calculation more self-consistently in order to get a lower critical temperature than the mean-field result.

In Fig. 10, the results of Fig. 7 for the superfluid critical temperature  $T_c$  (lower solid line) and Fig. 9 for the liquid-gas coexistence region (upper solid line) and the spinodal instability region (dashed line) have been combined in a single phase diagram. As explained above, we unfortunately cannot calculate the liquid-gas coexistence curve for  $T < 4.5$  MeV, but extrapolating the solid curve to lower temperatures and remembering that at  $T = 0$  the liquid phase gets stable at saturation density, it is clear that the coexistence curve will cross the superfluid  $T_c$  curve at  $n \sim n_0$ , i.e., as one would expect, homogeneous nuclear matter with pairing is stable above this density. From the results of Ref. [28] one can presume that the liquid-gas coexistence region will be slightly reduced below the superfluid critical temperature, but this

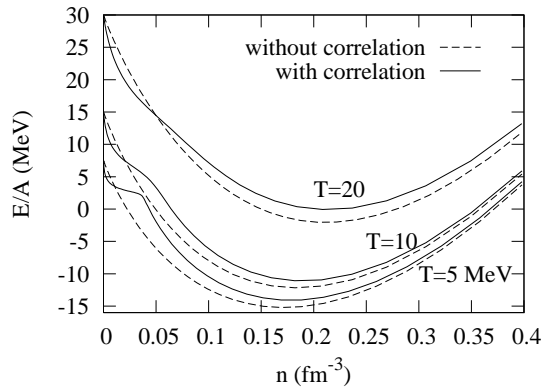


FIG. 11: Energy per nucleon as a function of density for different temperatures. Solid lines: with correlations; dashed lines: mean field results.

effect should be almost negligible in the case of symmetric nuclear matter considered here [28, 29]. At low densities, superfluid matter is never stable, because the superfluid  $T_c$  curve stays always below the coexistence curve.

The spinodal curve (dashed line) can be calculated until it reaches the superfluid region. From this we see that superfluid nuclear matter is metastable below  $n \sim 0.045 \text{ fm}^{-3}$  and above  $n \sim 0.1 \text{ fm}^{-3}$ . Note that on the low-density side, the density region where the gas phase is metastable is strongly increased by the correlations, especially when we approach the superfluid transition temperature. This confirms our expectation mentioned in the introduction that the correlations have a stabilizing effect. However, the BEC-BCS crossover lies still in the unstable region of the liquid-gas phase transition.

### C. Energy and entropy

The energy and the entropy can be obtained from the pressure with the help of the thermodynamic relations (21). Results for the energy per nucleon,  $E/A$ , and for the entropy per nucleon,  $S/A$ , for different temperatures are shown in Figs. 11 and 12. The corresponding mean-field results (dashed lines) are also shown for comparison. The results shown in Fig. 11 indicate that, for fixed temperature, the correlations shift the minimum of the energy per nucleon to slightly higher densities. Fortunately the change is very small, because otherwise we would have to readjust the parameters of the Gogny force, which gives the right saturation density and energy at zero temperature without correlations.

In the low-density region, where the deuterons and the nucleon-nucleon scattering states dominate, the energy per nucleon is lower than that the HF result. When the density is high, the correlation effect goes to zero and the energy per nucleon gets close to the mean-field result.

When the density approaches zero, both results go to

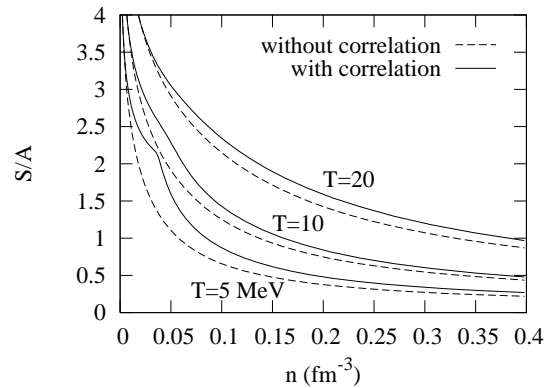


FIG. 12: Entropy per nucleon as a function of density for different temperatures. Solid lines: with correlations; dashed lines: mean field results.

the classical value of an ideal gas of nucleons,

$$\lim_{n \rightarrow 0} E/A = \frac{3}{2}T. \quad (27)$$

This is not surprising, since even the lowest temperature considered here,  $T = 5 \text{ MeV}$ , is still much higher than the deuteron binding energy so that almost all deuterons will be dissociated. However, the result (27) is also found at temperatures much lower than the deuteron binding energy. This is because, at finite temperature, the deuterons are always dissolved in the low-density limit. This is a consequence of the mass-action law and can easily be understood as follows: At low density, the chemical potential of the nucleons,  $\mu$ , gets strongly negative,  $\mu \ll -T$ . The chemical potential of the deuterons is  $2\mu$ , which is even more negative. So the nucleon density  $\propto e^{\mu/T}$  is much larger than the deuteron density  $\propto e^{2\mu/T}$ . Only at zero temperature, where the system remains a deuteron BEC at arbitrarily low densities, the energy per nucleon approaches  $-1.12 \text{ MeV}$  (half the deuteron binding energy) in the limit  $n \rightarrow 0$  [4].

The results for the entropy (cf. Fig. 12) have been calculated from Eq. (21) and show that, for fixed temperature, the entropy per nucleon decreases with increasing density. In the zero-density limit, the entropy per nucleon increases logarithmically, in agreement with the result for a classical ideal nucleon gas. As is clear from the discussion above, the correlations do not change this asymptotic behavior. At slightly larger values of the density, the correlations tend to increase the entropy.

## IV. SUMMARY

In this paper, we discussed the effect of pair correlations beyond the mean-field approximation in symmetric nuclear matter above the superfluid critical temperature. We include the effects of non-condensed pairs (deuterons) as well as the contribution of scattering states. For the

mean field, we use the Gogny effective interaction in order to get the right saturation properties of nuclear matter.

Starting from the single-particle Green's function within the Gogny HF approximation, we include the correlations in a perturbative way by considering in addition to the HF Green's function the diagram with one self-energy insertion, the self-energy being calculated in ladder approximation. This approximation scheme is analogous to the well-known NSR approach. However, in order to avoid double counting of the quasiparticle energy shift which is already accounted for by the Gogny mean field, we have to subtract the self-energy at the quasiparticle energy. This leads finally to the same formula for the density in terms of the in-medium scattering phase shifts as given in Ref. [6]. We use a separable Yamaguchi potential in order to get an analytical formula for the in-medium  $T$  matrix and the phase shifts.

Evaluating numerically these formulas for the density, we discussed the different density contributions in hot and dense nuclear matter and found that the nucleon-nucleon correlations are important in the low-temperature and low-density region ( $n < n_0$ ). The correlation effect on the superfluid critical temperature was discussed. The result interpolates between the critical temperature for Bose-Einstein condensation at low density and the BCS critical temperature at high density. We found that the maximum of the superfluid critical temperature decreases from 7.2 MeV (the value given in Ref. [6]) to 4.5 MeV when the effective mass  $m^*$  due to the Gogny mean field is taken into account.

Then we studied the liquid-gas phase transition in hot and dense nuclear matter with the help of the pressure calculated from the density. Especially at low density, we found that the boundaries of the coexistence and spinodal regions of the phase transition are shifted by the pair correlations. As we expected, the stable and metastable regions of the gas phase are strongly enlarged. In particular near the superfluid transition temperature, the gas phase stays metastable up to much higher densities if the correlations are taken into account. However, the correlations are not strong enough to suppress the liquid-gas transition. This could have been anticipated from the fact that the liquid-gas critical temperature is much higher than the superfluid one [28, 29]. Because of our perturbative treatment of the correlations, the critical temperature of the liquid-gas transition remains the same as within the mean field approximation.

Finally, we calculated the energy and entropy of nuclear matter from thermodynamic relations. The nucleon-nucleon correlations decrease the energy per nucleon in the low density region but increase it at high density. For the entropy, the correlations always give a positive contribution.

As mentioned before, our result for the critical temperature of liquid-gas phase transition is not affected by the pair correlations because they are treated only perturbatively. One should improve this by taking the correlations into account self-consistently. Then the correlations will

have some effect on the HF field and the critical temperature will change. The saturation point of nuclear matter, given correctly by the Gogny interaction within the HF approximation, may be changed, necessitating a readjustment of the parameters of the Gogny force.

Our equation of state is only valid for temperatures and densities above the superfluid critical temperature. In order to get a result which is valid in the whole temperature and density plane, one should introduce the pairing gap  $\Delta$  into the single-particle Green's functions. Some work in this direction has been done for nuclear matter [9], and quite elaborate theories have been developed for the BEC-BCS crossover in ultracold atomic Fermi gases [10]. We leave this for future study. Another important extension of the present work would be to consider the case of asymmetric nuclear matter and neutron matter, since these are of great importance for the study of neutron stars and their formation.

### Acknowledgments

We thank G. Röpke and J. Margueron for discussions and helpful remarks. M.J. acknowledges financial support from Université Paris-Sud 11 and from CNRS during his postdoctoral stays at Institut de Physique Nucléaire d'Orsay, where most of this work has been done. This work was supported in part by NSFC (grants 10805023 and 10975060) and by ANR (project NEXEN).

### Appendix: Derivation of the density formulas

In this Appendix we give a more transparent derivation of the density formulas (17), (18), and (19), which were initially derived in Refs. [5, 26]. For better readability, we will not write out the sum over  $\alpha = {}^3S_1, {}^1S_0$  and suppress the index  $\alpha$  in this appendix.

Let us recall the spectral representation of the  $T$  matrix,

$$T(k, k', K, \omega) = V(k, k') - \int \frac{d\omega'}{\pi} \frac{\text{Im} T(k, k', K, \omega')}{\omega - \omega' + i0}, \quad (28)$$

where  $\omega$  can be real or complex. Analogous dispersion relations exist for the self-energy  $\Sigma(p, \omega)$  and for the two-particle propagator  $J(K, \omega)$  defined in Eq. (13). Using Eq. (28), one can evaluate the frequency sum in Eq. (15), and one obtains the well-known expression for the imaginary part of the self-energy:

$$\text{Im} \Sigma(p, \omega) = \frac{3}{2} \int \frac{d^3 p'}{(2\pi)^3} \text{Im} T(k, k, K, \omega + \xi_{p'}) \times [f(\xi_{p'}) + g(\omega + \xi_{p'})]. \quad (29)$$

where  $\mathbf{k}$  and  $\mathbf{K}$  are the relative and total momenta as defined below Eq. (15).

The correlation correction to the density is given by

$$n_{corr} = -4T \sum_n \int \frac{d^3p}{(2\pi)^3} \frac{\Sigma(p, i\omega_n) - \text{Re} \Sigma(p, \xi_p)}{(i\omega_n - \xi_p)^2}. \quad (30)$$

If we use the spectral representation of  $\Sigma$ , the frequency sum can be evaluated with the result

$$n_{corr} = -4 \int \frac{d^3p}{(2\pi)^3} \mathcal{P} \int \frac{d\omega}{\pi} \text{Im} \Sigma(p, \omega) \frac{f(\omega) - f(\xi_p)}{(\omega - \xi_p)^2}, \quad (31)$$

where  $\mathcal{P}$  denotes the principal value. Inserting Eq. (29) into this expression, one obtains with the help of the relation  $f(\xi_p)f(\xi_{p'}) = g(\xi_p + \xi_{p'})[1 - f(\xi_p) - f(\xi_{p'})]$  and after some transformations

$$n_{corr} = -6 \int \frac{d^3p d^3p'}{(2\pi)^6} \mathcal{P} \int \frac{d\omega}{\pi} \text{Im} T(k, k, K, \omega) \times (1 - f(\xi_p) - f(\xi_{p'})) \frac{g(\omega) - g(\xi_p + \xi_{p'})}{(\omega - \xi_p - \xi_{p'})^2}. \quad (32)$$

The next step is to introduce the new variable  $\omega' = \xi_p + \xi_{p'}$  and to replace the integral over  $p'$  by an integral over  $\omega'$ . Then, using the imaginary parts of Eqs. (12) and (13), one can show that the resulting expression for  $n_{corr}$  can be rewritten as

$$n_{corr} = 6 \int \frac{d^3K}{(2\pi)^3} \mathcal{P} \int \frac{d\omega d\omega'}{\pi^2} \text{Im} \frac{1}{1 - J(K, \omega)} \times \text{Im} J(K, \omega') \frac{g(\omega) - g(\omega')}{(\omega - \omega')^2}. \quad (33)$$

With the help of the dispersion relations for the real

parts, this expression can be further reduced to

$$n_{corr} = 6 \int \frac{d^3K}{(2\pi)^3} \int \frac{d\omega}{\pi} g(\omega) \left( \text{Im} \frac{1}{1 - J} \frac{d}{d\omega} \text{Re} J - \text{Im} J \frac{d}{d\omega} \text{Re} \frac{1}{1 - J} \right) \quad (34)$$

(the arguments of  $J(K, \omega)$  have been suppressed for brevity). In order to express everything in terms of the in-medium scattering phase shifts  $\delta = -\text{Im} \ln(1 - J)$ , we notice that

$$\frac{d\delta}{d\omega} = \text{Im} \frac{1}{1 - J} \frac{d}{d\omega} \text{Re} J + \text{Re} \frac{1}{1 - J} \frac{d}{d\omega} \text{Im} J, \quad (35)$$

$$\text{Im} J \text{Re} \frac{1}{1 - J} = \sin \delta \cos \delta = \frac{1}{2} \sin 2\delta. \quad (36)$$

With these relations, Eq. (34) can be rewritten as

$$n_{corr} = 6 \int \frac{d^3K}{(2\pi)^3} \int \frac{d\omega}{\pi} g(\omega) \frac{d}{d\omega} (\delta - \frac{1}{2} \sin 2\delta). \quad (37)$$

The final step is to integrate by parts over  $\omega$  and to separate in the resulting integral the contributions of  $\omega > \omega_0(K)$  (scattering-state contribution  $n_{scatt}$ ) and  $\omega < \omega_0(K)$  (bound-state contribution  $n_{bound}$ ). The latter reduces to Eq. (18) since the phase shift below threshold is (see also Fig. 7 of Ref. [1])

$$\delta(K, \omega < \omega_0(K)) = \begin{cases} 0, & \text{if } K < K_{Mott}, \\ \pi\theta(\omega - \omega_b(K)), & \text{if } K > K_{Mott}. \end{cases} \quad (38)$$

- 
- [1] P. Nozières and S. Schmitt-Rink, *J. Low Temp. Phys.* **59** (1985) 195.  
[2] C.A. Regal, M. Greiner, D.S. Jin, *Phys. Rev. Lett.* **92** (2004) 040403.  
[3] M.W. Zwierlein, C.A. Stan, C.H. Schunck, S.M.F. Raupach, A.J. Kerman and W. Ketterle, *Phys. Rev. Lett.* **92** (2004) 120403.  
[4] M. Baldo, U. Lombardo, P. Schuck, *Phys. Rev. C* **52** (1995) 975.  
[5] M. Schmidt, G. Röpke, and H. Schulz, *Ann. Phys. (N.Y.)* **202** (1990) 57.  
[6] H. Stein, A. Schnell, T. Alm, and G. Röpke, *Z. Phys. A* **351** (1995) 295.  
[7] A. Rios, A. Polls, A. Ramos, and H. Mütter, *Phys. Rev. C* **78** (2008) 044314.  
[8] V. Somà and P. Božek, *Phys. Rev. C* **80** (2009) 025803.  
[9] P. Božek, *Nucl. Phys. A* **657** (1999) 187.  
[10] A. Perali, P. Pieri, L. Pisani, and G.C. Strinati, *Phys. Rev. Lett.* **92** (2004) 220404.  
[11] P. Pieri, L. Pisani, and G.C. Strinati, *Phys. Rev. B* **72** (2005) 012506.  
[12] P. Chomaz, M. Colonna, and J. Randrup, *Phys. Rep.* **389** (2004) 263.  
[13] B. Borderie and M.F. Rivet, *Prog. Part. Nucl. Phys.* **61** (2008) 551.  
[14] Y. G. Ma, *J. Phys. G: Nucl. Part. Phys.* **27** (2001) 2455; Y. G. Ma et al, *Phys. Rev. C* **71** (2005) 054606.  
[15] J.B. Elliott et al., *Phys. Rev. Lett.* **88** (2002) 042701; *Phys. Rev. C* **67** (2003) 024609.  
[16] S. Typel, G. Röpke, T. Klähn, D. Blaschke, and H.H. Wolter, *Phys. Rev. C* **81**, 015803 (2010).  
[17] J. Dechargé and D. Gogny, *Phys. Rev. C* **21** (1980) 1568.  
[18] J. Heyer, T.T.S. Kuo, J.P. Shen and S.S. Wu, *Phys. Lett. B* **202**, 465 (1988).  
[19] H. Song, G. Zheng, and R. Su, *J. Phys. G* **16** (1990) 1861.  
[20] J. Ventura, A. Polls, X. Viñas, S. Hernandez, and M. Pi, *Nucl. Phys. A* **545** (1992) 247c.  
[21] P. Ring and P. Schuck, *The Nuclear Many-Body Problem* (Springer-Verlag, Berlin, 1980).  
[22] A. Bouyssy and N. Vinh Mau, *Nucl. Phys. A* **224** (1974) 331; *ibid.* **229** (1974) 1.  
[23] M. F. Jiang, J. Heyer, S. D. Yang, T. T. S. Kuo, *Phys. Rev. Lett.* **61**(1988)38.  
[24] Y. Yamaguchi, *Phys. Rev.* **95** (1954) 1628.  
[25] A. L. Fetter and J. D. Walecka, *Quantum Theory of Many-Particle Systems* (McGraw-Hill, New York, 1971).

- [26] R. Zimmermann and H. Stolz, *Phys. Stat. Sol. (b)* **131** (1985) 151.
- [27] D.J. Thouless, *Ann. Phys. (N.Y.)* **10** (1960), 553.
- [28] H. Stein, C. Porthun, G. Röpke, *Eur. Phys. J. B* **2** (1998) 393.
- [29] R.K. Su, S.D. Yang, and T.T.S. Kuo, *Phys. Rev. C* **35** (1987) 1539.
- [30] G. Röpke, M. Schmidt, L. Münchow, H. Schulz, *Nucl. Phys. A* **399** (1983) 587.
- [31] L.G. Cao, U. Lombardo, and P. Schuck, *Phys. Rev. C* **74** (2006) 064301.
- [32] J.F. Berger, M. Girod, and D. Gogny, *Comput. Phys. Comm.* **63**, 365 (1991).
- [33] J. Margueron, Ph.D. thesis, Université Paris-Sud 11, 2001.
- [34] We prefer the D1 parametrization to the D1S one [32] because it allows us to compare our HF results with those of Ref. [20] and it gives a better compressibility of symmetric nuclear matter [33]. Anyway, since the effective mass  $m^*$  in D1 and D1S is almost the same, the results do not change qualitatively if we use D1S instead of D1.
- [35] Note also that the statement in Ref. [6], saying that Eq. (19) reduces to the NSR formula for the density after integration by parts if the term  $\propto \sin 2\delta_\alpha$  is omitted, is incorrect. In fact, the NSR formula involves a derivative  $d\delta/d\mu$  instead of  $d\delta/d\omega$  and therefore does not have a pole in the integrand even if that term is omitted. The term  $\propto \sin 2\delta_\alpha$  cannot be identified with the contribution of the subtraction of  $\Sigma(p, \xi_p)$  in Eq. (8).
- [36] Strictly speaking,  $n$  is not a function of  $\mu$  since it is not single-valued, as will be discussed later. In practice, we generate the curves in Figs. 4-12 by making a loop over the HF density and not over  $\mu$ .